Impact of peripheral myeloid cells on amyloid-β pathology in Alzheimer's disease–like mice

Stefan Prokop,[1]* Kelly R. Miller,[1]* Natalia Drost,[1] Susann Handrick,[1] Vidhu Mathur,[2,3] Jian Luo,[2,3] Anja Wegner,[1] Tony Wyss-Coray,[2,3] and Frank L. Heppner[1,4]

[1]Department of Neuropathology, Charité–Universitätsmedizin Berlin, 10117 Berlin, Germany
[2]Department of Neurology and Neurological Sciences, Stanford University School of Medicine, Stanford, CA 94305
[3]Center for Tissue Regeneration, Repair, and Restoration, VA Palo Alto Health Care System, Palo Alto, CA 94304
[4]Cluster of Excellence, NeuroCure, Charitéplatz 1, 10117 Berlin, Germany

Although central nervous system–resident microglia are believed to be ineffective at phagocytosing and clearing amyloid-β (Aβ), a major pathological hallmark of Alzheimer's disease (AD), it has been suggested that peripheral myeloid cells constitute a heterogeneous cell population with greater Aβ-clearing capabilities. Here, we demonstrate that the conditional ablation of resident microglia in CD11b-HSVTK (TK) mice is followed by a rapid repopulation of the brain by peripherally derived myeloid cells. We used this system to directly assess the ability of peripheral macrophages to reduce Aβ plaque pathology and therefore depleted and replaced the pool of resident microglia with peripherally derived myeloid cells in Aβ-carrying APPPS1 mice crossed to TK mice (APPPS1;TK). Despite a nearly complete exchange of resident microglia with peripheral myeloid cells, there was no significant change in Aβ burden or APP processing in APPPS1;TK mice. Importantly, however, newly recruited peripheral myeloid cells failed to cluster around Aβ deposits. Even additional anti-Aβ antibody treatment aimed at engaging myeloid cells with amyloid plaques neither directed peripherally derived myeloid cells to amyloid plaques nor altered Aβ burden. These data demonstrate that mere recruitment of peripheral myeloid cells to the brain is insufficient in substantially clearing Aβ burden and suggest that specific additional triggers appear to be required to exploit the full potential of myeloid cell–based therapies for AD.

CORRESPONDENCE
Frank L. Heppner:
frank.heppner@charite.de

Abbreviations used: Aβ, amyloid-β; aCSF, artificial cerebrospinal fluid; Act, actin; AD, Alzheimer's disease; CNS, central nervous system; CTF, C-terminal fragment; GCV, ganciclovir; GFP, enhanced green fluorescent protein; icv, intracerebroventricular(ly); qPCR, quantitative PCR; TK, CD11b-HSVTK.

Microglia reactivity to amyloid-β (Aβ) plaques is a key feature of Alzheimer's disease (AD) pathology, but the exact nature of this cellular immune response and impact on disease pathogenesis and progression is still far from clear (Prokop et al., 2013). During the progression of Aβ pathology in AD-like mouse models, microglia exhibit a reduction in cellular functions like phagocytosis and response to injury (Krabbe et al., 2013), and depletion of microglia for up to 30 d in two mouse models of AD had no major impact on development or progression of Aβ pathology (Grathwohl et al., 2009), suggesting that microglia are inefficient at managing the increasing Aβ load. In contrast, there are examples in which modulation of the microglia response toward Aβ did have a major impact on disease progression (vom Berg et al., 2012; Heneka et al., 2013; Chakrabarty et al., 2015; Guillot-Sestier et al., 2015). Further complicating the quest for understanding the role of microglia in AD is the fact that peripheral

*S. Prokop and K.R. Miller contributed equally to this paper.
S. Prokop's present address is Dept. of Pathology and Laboratory Medicine, Hospital of the University of Pennsylvania, Philadelphia, PA 19104.
K.R. Miller's present address is Center for Neurodegenerative Disease Research, Dept. of Pathology and Laboratory Medicine, Perelman School of Medicine, University of Pennsylvania, Philadelphia, PA 19104.
A. Wegner's present address is School of Cellular and Molecular Medicine, University of Bristol, Bristol BS8 1TD, England, UK.

The Rockefeller University Press $30.00
J. Exp. Med. 2015 Vol. 212 No. 11 1811–1818
www.jem.org/cgi/doi/10.1084/jem.20150479

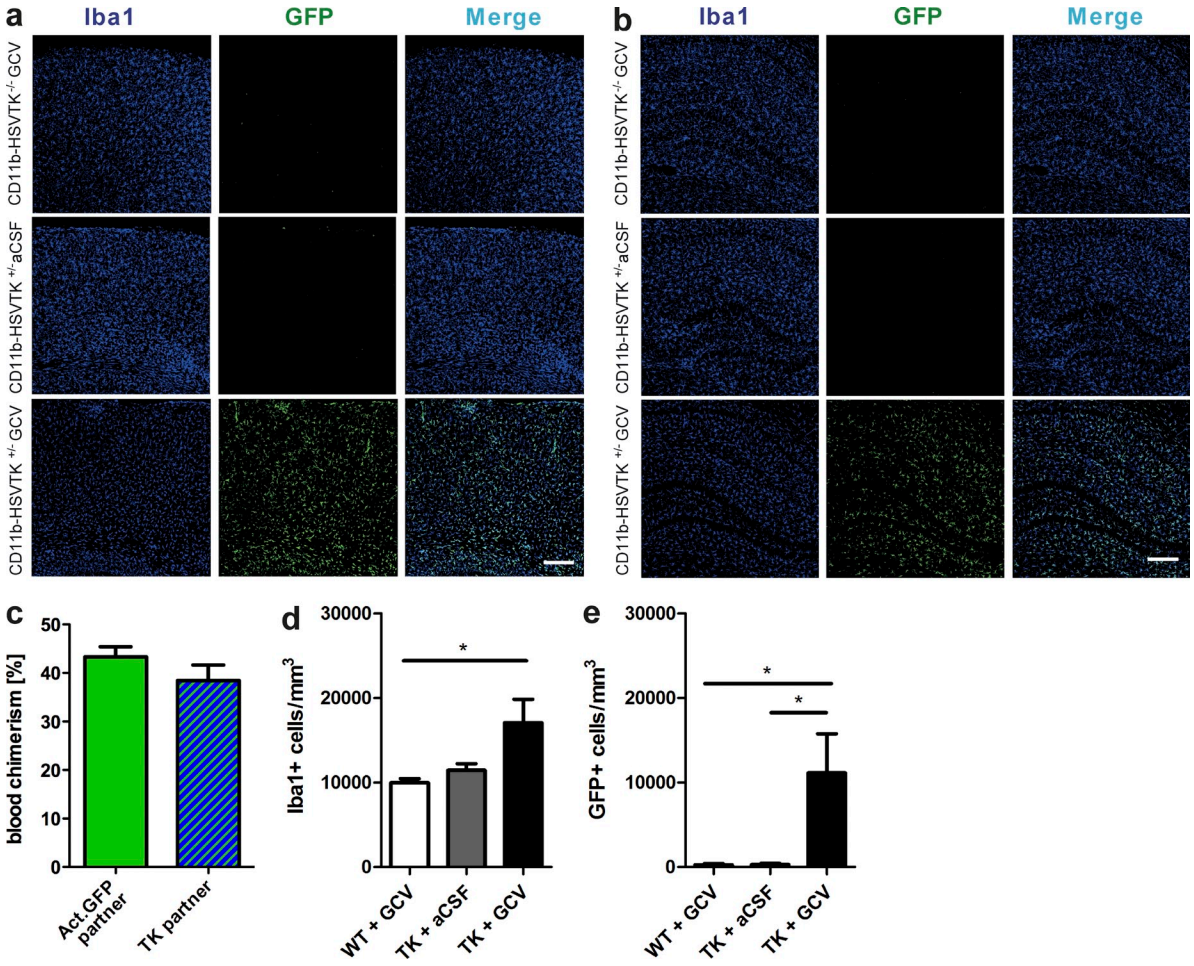

Figure 1. Peripheral origin of repopulating myeloid cells in nonchimeric microglia-depleted parabiotic mice. TK and Act.GFP mice were surgically connected to establish a joined circulatory system. Upon establishment of blood chimerism in both partners (2 wk), icv GCV was administered to the TK partners for 10 d to deplete microglia. Mice were sacrificed 24 d after starting GCV treatment. (a and b) Representative images of GFP-positive cells (middle columns) in microglia-depleted (GCV-treated) TK mice (bottom rows), WT controls (top rows), or non-microglia–depleted aCSF-treated TK controls (middle rows). Shown are cortical (a) or hippocampal (b) brain regions stained for Iba1 (left columns) or GFP (middle columns), as well as merged images (right columns). Bars, 200 µm. (c) Flow cytometric analysis of GFP$^+$ cells in blood of parabiotic pairs. (d and e) Stereological quantification of Iba1-positive cells (d; *, P = 0.03; n = 5 per group) and GFP-positive cells (e; *, P = 0.02; n = 5 per group) in brains of mice described in a–c. All data are displayed as mean ± SEM.

myeloid cells can enter the central nervous system (CNS) under certain conditions (Ajami et al., 2007; Mildner et al., 2011) and contribute to the immune response toward Aβ deposits (Stalder et al., 2005). The notion that newly recruited myeloid cells may be better effector cells than the dysfunctional resident microglia to combat Aβ deposits has been supported by studies claiming or demonstrating that reduced recruitment of myeloid cells enhances AD-like pathology (Simard et al., 2006; Mildner et al., 2011; Naert and Rivest, 2011) and, similarly, that enhanced recruitment of myeloid cells can be beneficial for the clearance of Aβ pathology (Town et al., 2008). To directly test the hypothesis that peripheral myeloid cells are better Aβ-combatting cells than resident microglia, we used an experimental mouse model that allows for the exchange of resident microglia by peripherally derived myeloid cells upon conditional depletion of these CNS-resident cells (Varvel et al., 2012). Our data reveal that exchanging the microglia population with peripheral macrophages fails to reduce Aβ pathology and, importantly, that infiltrating myeloid cells show no targeted response to Aβ plaques.

RESULTS AND DISCUSSION

Peripheral origin of CNS-repopulating myeloid cells in microglia-depleted CD11b-HSVTK (TK) mice

To demonstrate the origin of the cells repopulating the microglia-depleted brain in TK mice (Varvel et al., 2012) without the bias and side effects of bone marrow chimerism, we performed isochronic parabiosis experiments, in which TK mice were paired with Actin.enhanced green fluorescent protein (Act.GFP) partners (for experimental details see Fig. 1). After successful establishment of a joined blood compartment, demonstrated by a blood chimerism of ∼40% (Fig. 1 c), we achieved the exchange of resident microglia in the TK

transgene–expressing partner by intracerebroventricular (icv) application of ganciclovir (GCV) for 10 d, followed by 2 wk of no treatment (Fig. 1). Although the application of GCV into wild-type control mice and the application of artificial cerebrospinal fluid (aCSF) in TK mice did not lead to a significant influx of GFP-positive peripheral myeloid cells into the brain (Fig. 1, a, b, and e), in TK mice treated with GCV (resulting in depletion of endogenous microglia) we observed a robust increase in Iba1-positive cells (Fig. 1 d), as described previously (Varvel et al., 2012). Consistent with the degree of chimerism, a substantial percentage of the CNS-infiltrating cells were GFP positive (Fig. 1, a, b, and e), indicating their peripheral origin, and were observed evenly distributed throughout the parenchyma (Fig. 1, a and b). These data demonstrate that in the TK mouse model, depletion of resident microglia is followed by a rapid repopulation by peripherally derived myeloid cells in the absence of additional stimuli, such as bone marrow chimerism or whole brain irradiation.

No recruitment of peripherally derived myeloid cells to Aβ plaques

To exchange the resident microglia pool with peripheral myeloid cells in an Aβ-carrying AD-like mouse model, we generated APPPS1;$TK^{+/-}$ mice by crossing APPPS1 (Radde et al., 2006) to TK mice (Heppner et al., 2005). 28 d after a 10-d GCV regimen to deplete endogenous microglia, we observed a repopulation of the microglia niche by Iba1-positive cells in APPPS1;$TK^{+/-}$ mice (Fig. 2 a). The newly recruited myeloid cells in APPPS1;$TK^{+/-}$ mice were present at numbers comparable with the endogenous microglia cells in similarly GCV-treated APPPS1;$TK^{-/-}$ mice (Fig. 2 b) and untreated APPPS1 mice (not depicted). In addition, these cells exhibited a distinct morphology characterized by broader, more rod-shaped cell bodies than the ramified resident microglia (Fig. 2 a). Furthermore, the newly repopulating cells were evenly distributed throughout the tissue, as has been previously described for the repopulation paradigm in the non-AD context (Varvel et al., 2012). Strikingly, however, the obvious clustering of resident microglia around Aβ deposits normally observed in the AD brain and AD mouse models, including the nonrepopulated APPPS1;$TK^{-/-}$ control mice used in this study, was not apparent in APPPS1;$TK^{+/-}$ mice harboring peripheral myeloid cells in the brain (Fig. 2 c), suggesting that Aβ plaques serve as an insufficient stimulus to induce a targeted response by infiltrating macrophages. Quantitative PCR (qPCR) analysis of RNA isolated from cerebral hemispheres of APPPS1;$TK^{+/-}$ and APPPS1;$TK^{-/-}$ mice revealed a significant down-regulation of the gene hexosaminidase B (*Hexb*) and the purinergic receptor *P2ry12* (Fig. 2 d), both of which have been shown to be significantly enriched in CNS-resident microglia compared with peripheral macrophages (Hickman et al., 2013), thus confirming the successful depletion of resident microglia and replacement by peripheral myeloid cells. In contrast, the common microglia and macrophage genes *CD11b* and *Cx3cr1* remained unchanged (Fig. 2 d), which is well in line with detecting equivalent numbers of stereologically quantified Iba1-positive cells in repopulated, APPPS1;$TK^{+/-}$and nonrepopulated, APPPS1;$TK^{-/-}$ mice (Fig. 2 b). Interestingly, *Trem2*, a gene recently identified as a risk factor for AD (Guerreiro et al., 2013; Jonsson et al., 2013), also remained unchanged upon peripheral macrophage infiltration, suggesting that both resident microglia and peripheral myeloid cells can contribute to TREM2 protein expression in the brain, an issue which has been discussed controversially (Frank et al., 2008; Ulrich et al., 2014; Jay et al., 2015).

Unaltered Aβ pathology in the presence of peripherally derived myeloid cells

Surprisingly, the exchange of endogenous microglia with peripheral myeloid cells did not affect cerebral amyloid pathology, as judged by stereological quantification of Aβ plaque burden (Fig. 2, e and f). Similarly, the amount of Congo red–positive plaques was also not altered in the presence of peripheral macrophages (Fig. 2, g and h). In line with these findings, biochemical analyses revealed unchanged levels of soluble and insoluble as well as total Aβ species (Fig. 2 i) in brains of APPPS1;$TK^{+/-}$ mice harboring peripheral myeloid cells when compared with APPPS1;$TK^{-/-}$ mouse brains comprising resident microglia. Finally, there was also no major effect on APP processing, as judged by assessing the amounts of APP, $APP_{CTF\beta}$, and $APP_{CTF\alpha}$ (CTF, C-terminal fragment) by means of Western blotting (Fig. 2 j). Although it was unexpected that the exchange of endogenous microglia with large numbers of peripheral myeloid cells had no effect on Aβ pathology, this result is less surprising given the failure of infiltrating macrophages to associate with Aβ plaques (Fig. 2 c). Given that astrocytes are present in this model and capable of producing chemokines (Liu et al., 2014), along with some remaining endogenous microglia, this lack of attraction to plaques by peripherally derived myeloid cells may be because Aβ plaques do not represent a sufficient or appropriate innate immune-activating stimulus. However, this question deserves further investigation in future experiments.

Passive Aβ vaccination is insufficient to direct peripherally derived myeloid cells to amyloid plaques

To provide a more stringent setting in which to test the Aβ-clearing abilities of infiltrating myeloid cells, we sought to actively recruit the cells toward the Aβ plaques by treating animals with the anti-Aβ antibody Ab9 upon myeloid cell repopulation (Levites et al., 2006), which has been shown to direct the myeloid cell response toward amyloid deposits (Wang et al., 2011). After microglia depletion in APPPS1;$TK^{+/-}$ mice and identical treatment of respective APPPS1;$TK^{-/-}$ control mice, GCV administration was stopped. During a subsequent 4-wk time period in which the newly recruited peripheral myeloid cells were present in the brain, mice received a series of six intraperitoneal injections of Ab9 or respective isotype control antibodies; the former regimen has been found to confer a reduction in amyloid burden in Aβ-carrying mice (not depicted). Again, we observed similar

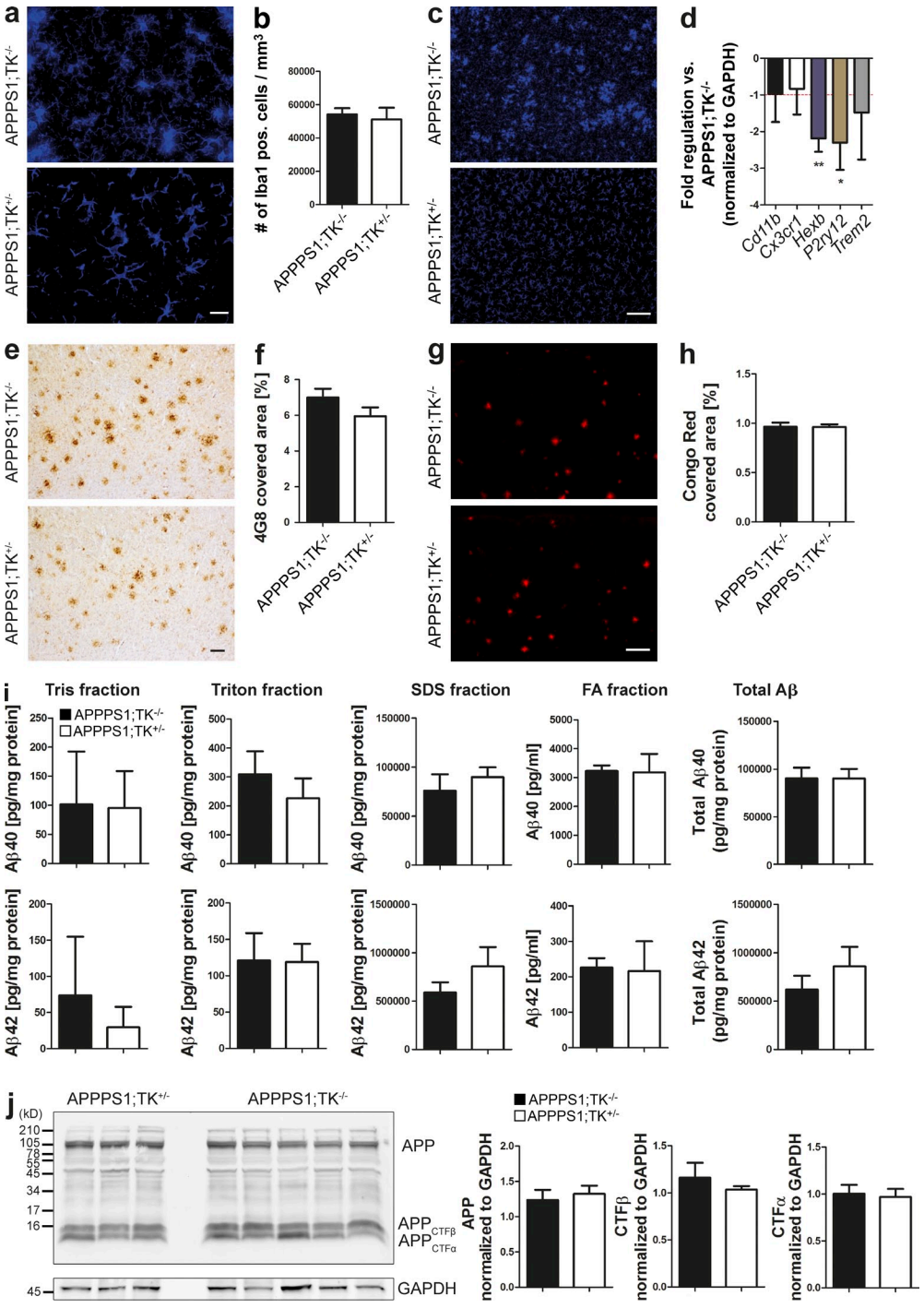

Figure 2. Peripheral myeloid cells do not affect Aβ pathology in microglia-depleted APPPS1;TK$^{+/-}$ mice. (a) Representative images of Iba1 immunohistochemistry (blue) in peripheral myeloid cell–repopulated APPPS1;TK$^{+/-}$ mice (bottom) and similarly GCV-treated APPPS1;TK$^{-/-}$ control mice (top). (b) Stereological quantification of Iba1-positive cells (n = 5–8 per group). (c) Overview images of Iba1 immunohistochemistry (blue). (d) qPCR analysis of *Cd11b*, *Cx3cr1*, *Hexb*, *P2ry12*, and *Trem2* from whole brain tissue of APPPS1;TK$^{+/-}$ mice compared with APPPS1;TK$^{-/-}$ controls (*, P = 0.03; **, P = 0.007; n = 6 per group). (e) Representative images of 4G8 immunohistochemistry. (f) Stereological quantification of the area covered by 4G8-positive plaques (n = 6–9 per group). (g and h) Congo red staining (g) and stereological quantification (h) of the area covered by Congo red–positive plaques (n = 6–9 per group). Bars: (a) 20 µm; (c, e, and g) 100 µm. (i) Amount of soluble and insoluble Aβ40 and Aβ42 and total Aβ40 and Aβ42 calculated from individual fractions measured by Meso Scale Diagnostics (measurements performed in duplicate from n = 5 biological replicates per group). (j) Representative Western blot images of APP, $APP_{CTF\beta}$, and $APP_{CTF\alpha}$ in SDS fractions from brain homogenates described in i (6E10 detection; left) and representative quantification of Western blots (right; result representative for four independent experiments). All p-values >0.05 unless otherwise stated. All data are represented as mean ± SEM. All mice were treated icv for 10 d with GCV followed by a 28-d period without GCV administration.

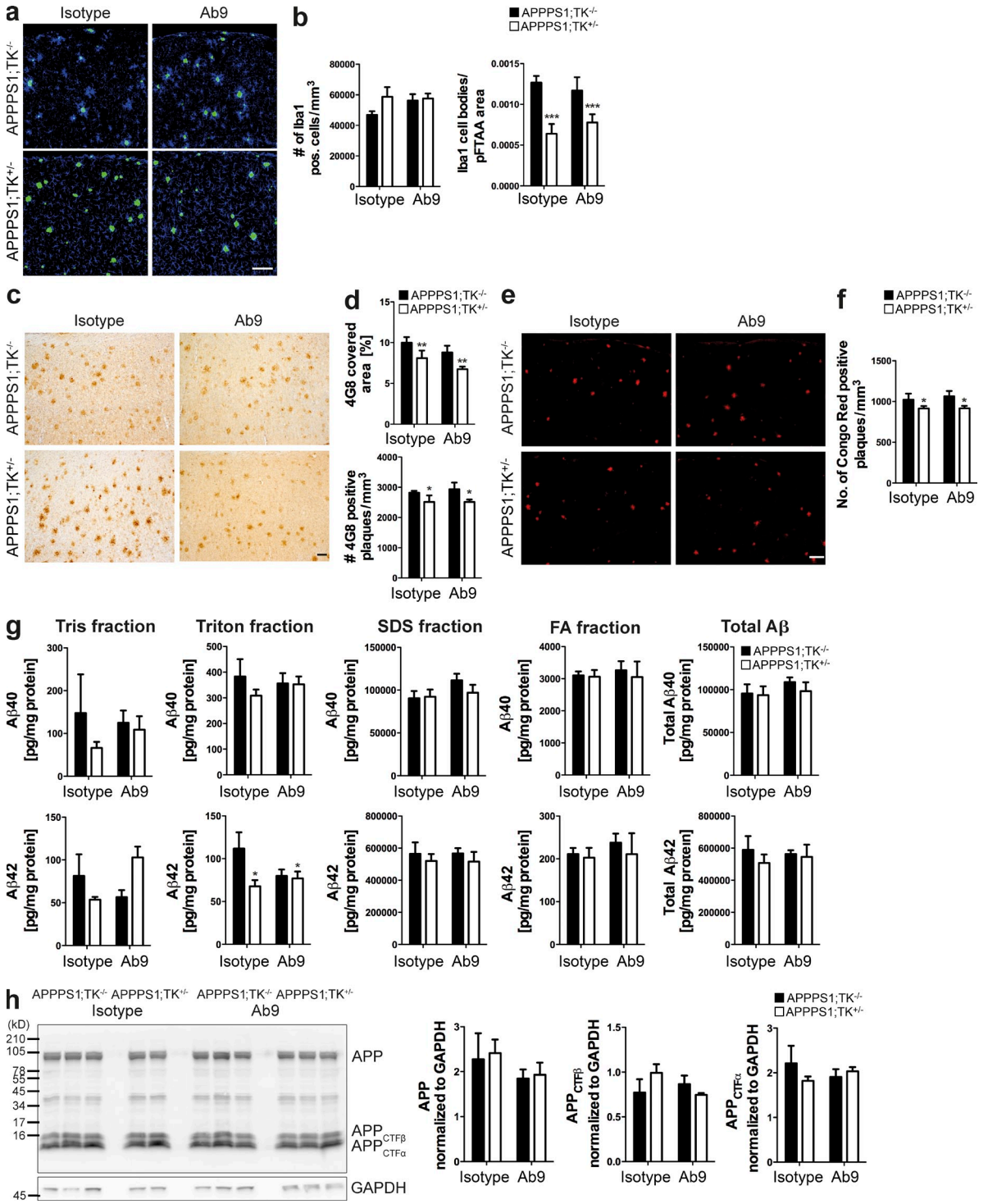

Figure 3. Anti-Aβ antibodies fail to specifically promote plaque association or clearance by peripheral myeloid cells. (a) Representative images of Iba1 immunohistochemistry (blue) combined with pFTAA staining (green) are shown. (b) Stereological quantification of number of Iba1-positive cells (left; $n = 5–6$ per group) and quantification of Iba1-positive cell bodies per pFTAA area (right; $n = 5–6$ per group; ***, P = 0.0005). (c and e) Representative images of 4G8 immunohistochemistry (c) and Congo red staining (e). (a, c, and e) Bars, 100 µm. (d) Stereological quantification of the area covered by 4G8-positive plaques (top; **, P = 0.009) and number of 4G8-positive plaques (bottom; *, P = 0.02; $n = 5–7$ per group). (f) Stereological quantification of the number of Congo red–positive plaques (*, P = 0.02; $n = 5–7$ per group). (g) Amount of soluble and insoluble Aβ40 and Aβ42 and total Aβ40 and Aβ42 calculated from individual protein fractions (*, P = 0.04; measurements performed in duplicate from $n = 5–7$ biological replicates per group). (h) Representative image of Western blot analyses of APP, $APP_{CTFβ}$, and $APP_{CTFα}$ in SDS-extracted brain fractions (APPct detection; left) and representative quantification of Western blots (right; result representative of six independent experiments). All data are represented as mean ± SEM.

numbers of Iba1-positive cells in repopulated APPPS1;TK$^{+/-}$ and nonrepopulated APPPS1;TK$^{-/-}$ control mice treated with Ab9 or isotype control antibodies (Fig. 3, a and b, left). As in the previous experiment (Fig. 2 c), there was no obvious clustering of the newly recruited cells around cerebral Aβ deposits in isotype antibody–treated repopulated mice compared with identically treated nonrepopulated, APPPS1 mice (Fig. 3 a, left). Quantification of the number of plaque-associated Iba1-positive cells revealed significantly fewer cells per plaque (Fig. 3 b, right). Notably, treatment with Aβ-specific antibodies failed to recruit more Iba1-positive cells to the plaques in repopulated mice (Fig. 3, a and b, right). Although we observed a reduction in the number and area covered by Aβ plaques in APPPS1;TK$^{+/-}$ mice harboring peripheral myeloid cells (Fig. 3, c and d), this difference was not specific for Ab9 treatment, as isotype-treated APPPS1;TK$^{+/-}$ mice showed a similar reduction. Similarly, there was also a reduction in Congo red–positive plaques in myeloid cell repopulated APPPS1;TK$^{+/-}$ mice that did not differ between isotype and Ab9 treatment (Fig. 3, e and f), suggesting that nonspecific stimulation of peripheral myeloid cells served to mediate a modestly improved amyloid clearance activity of these cells compared with endogenous microglia. In line with these very mild changes in plaque burden, there was no major effect on soluble and insoluble as well as total Aβ levels in respective biochemical analyses (Fig. 3 g) and no impact on APP processing, as judged by levels of APP, $APP_{CTF\beta}$, and $APP_{CTF\alpha}$ (Fig. 2 h).

Conclusion

Although the presence of peripheral myeloid cells in the CNS for 1 mo may simply be too short a timeframe to see a substantial impact of those newly recruited cells on Aβ pathology, in this issue, Varvel et al. demonstrate that the extended presence of peripheral myeloid cells in the AD-like brain does not suffice to reduce Aβ deposition. Moreover, it is not surprising that we did not observe major differences in pathology given the fact that peripherally derived myeloid cells failed to associate with Aβ deposits even in the presence of Aβ-specific antibodies. The mild, but not statistically significant effect on Aβ plaque–covered area in repopulated anti-Aβ antibody and isotype-treated mice suggests that additional priming of peripheral myeloid cells or exposure to Aβ before entering the brain may be required to target these cells to Aβ deposits as an essential prerequisite to induce an efficient reduction in Aβ burden. In line with this notion, one has to keep in mind that previously published studies reporting effects of infiltrating macrophages on Aβ pathology used genetic models to either prevent recruitment of peripheral myeloid cells, e.g., by deficiency in CCR2 (Mildner et al., 2011; Naert and Rivest, 2011), or enhance the influx of these cells to the brain (Town et al., 2008). In addition to modulating the recruitment to the brain, these genetic modifications also impact the activation status of the myeloid cell population (including the resident microglia), which thus can have a major impact on Aβ pathology by itself, irrespective of an increased recruitment of peripheral myeloid cells to the CNS. Finally, one can also speculate that Aβ plaques are not sufficiently stimulating to engage myeloid cells but that these cells rather respond to tissue damage associated with earlier stages of plaque development, suggesting that recruitment of peripheral macrophages to the brain may only be effective at very early stages of disease. It will be thus of utmost importance to better understand the differences between endogenous microglia and peripheral macrophages and to further dissect the specific factors involved in attracting myeloid cells to Aβ plaques and in efficient clearance of Aβ deposits to develop novel myeloid cell–based therapeutic strategies for the treatment of AD.

MATERIALS AND METHODS

Animals and surgery. APPPS1 transgenic mice (Radde et al., 2006) were provided by M. Jucker (University of Tübingen, Tübingen, Germany). Male APPPS1$^{+/-}$ mice were crossed to female TK mice (Heppner et al., 2005) to generate APPPS1;TK$^{+/-}$ animals and APPPS1;TK$^{-/-}$ littermate controls. All animals were housed under specific pathogen–free conditions on a 12-h light/dark cycle. Food and water were provided ad libitum. All animal experiments were conducted in accordance with animal welfare acts and were approved by the regional offices for health and social services in Berlin (LaGeSo). Microglia depletion was achieved in all mice harboring the TK transgene as described previously (Grathwohl et al., 2009), with modifications. In brief, Cymevene (Roche; 2.5 mg/ml at a flow rate of 1 µl/h) was administered icv for 10 d using a mini-osmotic pump (model 2001; Alzet). Cymevene treatment was ceased by removal of osmotic pumps under isoflurane anesthesia via a small incision in the flank without disruption of the cannula. After 10 d of GCV (Cymevene) treatment, APPPS1;TK$^{+/-}$ mice and APPPS1;TK$^{-/-}$ control mice received a regimen of six intraperitoneal injections of 500 µg of either $Aβ_{1–16}$-specific clone Ab9 antibody (QED Bioscience Inc.) or total nonspecific mouse IgG (Equitech Bio) that was purified via protein G column (GE Healthcare). All animals were aged ∼155 d at the start of experiments.

Parabiosis experiments were performed as previously described (Villeda et al., 2011), with modifications. In brief, 10 d before surgical joining of mice, icv cannula attached to mini-osmotic pumps containing aCSF were implanted into the lateral ventricles of wild-type or TK partners. 2 wk after wild-type or TK mice were joined with Act.GFP partners, aCSF-containing mini-osmotic pumps were exchanged through a small incision in the flank with mini-osmotic pumps containing GCV or aCSF. GCV (Roche; 2.5 mg/ml at a flow rate of 1 µl/h) or aCSF was administered for 10 d, and mice were sacrificed 14 d after the cessation of GCV (or aCSF; 24 d after the start of GCV treatment).

Tissue processing. For histological, biochemical, and RNA preparations, animals were deeply anesthetized using a ketamine (100 mg/kg) and xylazine (10 mg/kg) cocktail and transcardially perfused with sterile PBS, pH 7.4. Brains were rapidly removed and divided in half sagittally. The hemisphere ipsilateral to the cannula injection site was rapidly frozen in liquid nitrogen and stored at −80°C until processing. The rostral portion of the brain hemisphere was processed for biochemical analysis, and the caudal portion was used for RNA isolation. The contralateral brain hemisphere was immersed in 4% formaldehyde and stored at 4°C for 24 h. Subsequently, the tissue was transferred to a 30% sucrose solution until sectioning.

Gene expression analysis. RNA was isolated using TriFast (PEQLAB Biotechnology). RNA concentration was determined and purity assessed using an Infinite 200 microplate reader (Tecan). 1 µg RNA per sample was reverse transcribed to generate cDNA (Quanti Tect Reverse Transcription kit; QIAGEN). All qPCR was performed using a 7900HT Fast Real-Time PCR System (Applied Biosystems) using cataloged TaqMan assays. Normalization was performed in relation to *Gapdh*. Specificity of amplification was assessed by melting curve analysis. Data analysis was performed manually using the ΔΔCt method. Positive fold change values between zero and one were converted to fold regulation by calculating the reciprocal.

Histology. Formalin-fixed and sucrose-treated brain hemispheres contralateral to the cannula injection site were frozen at −25°C and cryosectioned coronally at 30 µm. Tissue sections were collected throughout the entire rostrocaudal extent of the brain and stored at 4°C until staining. Immunohistochemistry and subsequent stereological analyses were performed on 10–12 systematically randomly sampled sections collected at 180-µm intervals for each marker analyzed. Stereological quantification of $Iba1^+$ cells and Congo red^+ plaques were performed using the Optical Fractionator method (MicroBrightField). Quantification of $4G8^+$ plaques was performed using the Area Fraction fractionator method (MicroBrightField). Plaque-associated microglia were quantified in five sections per sample at 200 magnification in sections double-labeled for Iba1 and pFTAA. 5–10 plaques per image were randomly selected for analysis and the number of $Iba1^+$ cells around each plaque was counted and normalized to the total pFTAA area covered by the selected plaques. Amyloid staining was performed using Congo red (Carl Roth) and pFTAA luminescent–conjugated oligothiophene solution (gift of P. Nilsson, Linköping University, Linköping, Sweden). Immunohistochemistry was performed on free-floating sections using primary antibodies against Iba1 (1:500; Wako Pure Chemical Industries) and 4G8 (1:1,000; Covance). Antibody binding was visualized using appropriate peroxidase-conjugated secondary antibodies (1:100; Dianova) and diaminobenzidine (DAB) substrate (Sigma-Aldrich) or Alexa Fluor–conjugated secondary antibodies (1:300; Invitrogen). Light microscopy and stereology were performed using a Stereo Investigator system (MicroBrightField) and DV-47d camera (MicroBrightField) mounted on a BX53 microscope (Olympus). Fluorescence imaging was performed using an XM10 monochrome fluorescence charge-coupled device camera (Olympus).

Biochemical analysis. For analysis of soluble and insoluble Aβ levels, snap-frozen brain hemispheres were subjected to a four-step extraction protocol (Kawarabayashi et al., 2001). Protein amount of Aβ40 and Aβ42 in each fraction was quantified using the Meso Scale ELISA system (V-PLEX Aβ Peptide Panel 1 [6E10] kit; Meso Scale Discovery). Expression levels of endogenous mouse and transgenic human APP and major C-terminal cleavage products of APP (CTFα and CTF) were assessed by Western blot analysis using the APPct antibody (A8717; Sigma-Aldrich) and quantified by densitometric scanning. GAPDH (MAB 374; Merck) was used as an internal control for normalization.

Statistical analysis. Student's *t* tests were used to make pairwise comparisons when two experimental groups were compared. Two-way ANOVA was performed to determine whether significant differences existed among comparisons of three or more groups. Post hoc pairwise comparisons were performed using Bonferroni's multiple comparison test. A p-value of 0.05 or less was adopted as a threshold for assigning statistical significance. For gene expression analysis of qPCR array data, p-values were calculated based on a Student's *t* test of the replicate $2\text{-}\Delta Ct$ values for each gene in the control and treatment groups.

We thank Claudia Hempt, Alexander Haake, and Claire Gelhaar for excellent technical assistance.

This work was supported by grants from the Deutsche Forschungsgemeinschaft (SFB TRR 43, NeuroCure Exc 257) and from the Berlin Institute of Health (BIH; Collaborative Research Grant) to F.L. Heppner and from the Federal Ministry of Education and Research (DLR/BMBF; Kompetenznetz Degenerative Demenzen) to F.L. Heppner and S. Prokop. T. Wyss-Coray was supported by a NeuroCure Visiting Fellowship.

The authors declare no competing financial interests.

Author contributions: S. Prokop, K.R. Miller, and F.L. Heppner conceived the study. S. Prokop and K.R. Miller performed experiments, analyzed data, and co-wrote the manuscript. N. Drost, S. Handrick, and A. Wegner performed stereological analyses of tissue sections, whereas K.R. Miller, V. Mathur, J. Luo, and T. Wyss-Coray performed parabiosis experiments. F.L. Heppner critically edited the manuscript and directed the study.

Submitted: 16 March 2015
Accepted: 16 September 2015

REFERENCES

Ajami, B., J.L. Bennett, C. Krieger, W. Tetzlaff, and F.M. Rossi. 2007. Local self-renewal can sustain CNS microglia maintenance and function throughout adult life. *Nat. Neurosci.* 10:1538–1543. http://dx.doi.org/10.1038/nn2014

Chakrabarty, P., A. Li, C. Ceballos-Diaz, J.A. Eddy, C.C. Funk, B. Moore, N. DiNunno, A.M. Rosario, P.E. Cruz, C. Verbeeck, et al. 2015. IL-10 alters immunoproteostasis in APP mice, increasing plaque burden and worsening cognitive behavior. *Neuron.* 85:519–533. http://dx.doi.org/10.1016/j.neuron.2014.11.020

Frank, S., G.J. Burbach, M. Bonin, M. Walter, W. Streit, I. Bechmann, and T. Deller. 2008. TREM2 is upregulated in amyloid plaque-associated microglia in aged APP23 transgenic mice. *Glia.* 56:1438–1447. http://dx.doi.org/10.1002/glia.20710

Grathwohl, S.A., R.E. Kälin, T. Bolmont, S. Prokop, G. Winkelmann, S.A. Kaeser, J. Odenthal, R. Radde, T. Eldh, S. Gandy, et al. 2009. Formation and maintenance of Alzheimer's disease β-amyloid plaques in the absence of microglia. *Nat. Neurosci.* 12:1361–1363. http://dx.doi.org/10.1038/nn.2432

Guerreiro, R., A. Wojtas, J. Bras, M. Carrasquillo, E. Rogaeva, E. Majounie, C. Cruchaga, C. Sassi, J.S. Kauwe, S. Younkin, et al. Alzheimer Genetic Analysis Group. 2013. TREM2 variants in Alzheimer's disease. *N. Engl. J. Med.* 368:117–127. http://dx.doi.org/10.1056/NEJMoa1211851

Guillot-Sestier, M.V., K.R. Doty, D. Gate, J. Rodriguez Jr., B.P. Leung, K. Rezai-Zadeh, and T. Town. 2015. Il10 deficiency rebalances innate immunity to mitigate Alzheimer-like pathology. *Neuron.* 85:534–548. http://dx.doi.org/10.1016/j.neuron.2014.12.068

Heneka, M.T., M.P. Kummer, A. Stutz, A. Delekate, S. Schwartz, A. Vieira-Saecker, A. Griep, D. Axt, A. Remus, T.C. Tzeng, et al. 2013. NLRP3 is activated in Alzheimer's disease and contributes to pathology in APP/PS1 mice. *Nature.* 493:674–678. http://dx.doi.org/10.1038/nature11729

Heppner, F.L., M. Greter, D. Marino, J. Falsig, G. Raivich, N. Hövelmeyer, A. Waisman, T. Rülicke, M. Prinz, J. Priller, et al. 2005. Experimental autoimmune encephalomyelitis repressed by microglial paralysis. *Nat. Med.* 11:146–152. http://dx.doi.org/10.1038/nm1177

Hickman, S.E., N.D. Kingery, T.K. Ohsumi, M.L. Borowsky, L.C. Wang, T.K. Means, and J. El Khoury. 2013. The microglial sensome revealed by direct RNA sequencing. *Nat. Neurosci.* 16:1896–1905. http://dx.doi.org/10.1038/nn.3554

Jay, T.R., C.M. Miller, P.J. Cheng, L.C. Graham, S. Bemiller, M.L. Broihier, G. Xu, D. Margevicius, J.C. Karlo, G.L. Sousa, et al. 2015. TREM2 deficiency eliminates $TREM2^+$ inflammatory macrophages and ameliorates pathology in Alzheimer's disease mouse models. *J. Exp. Med.* 212:287–295. http://dx.doi.org/10.1084/jem.20142322

Jonsson, T., H. Stefansson, S. Steinberg, I. Jonsdottir, P.V. Jonsson, J. Snaedal, S. Bjornsson, J. Huttenlocher, A.I. Levey, J.J. Lah, et al. 2013. Variant of TREM2 associated with the risk of Alzheimer's disease. *N. Engl. J. Med.* 368:107–116. http://dx.doi.org/10.1056/NEJMoa1211103

Kawarabayashi, T., L.H. Younkin, T.C. Saido, M. Shoji, K.H. Ashe, and S.G. Younkin. 2001. Age-dependent changes in brain, CSF, and plasma amyloid β protein in the Tg2576 transgenic mouse model of Alzheimer's disease. *J. Neurosci.* 21:372–381.

Krabbe, G., A. Halle, V. Matyash, J.L. Rinnenthal, G.D. Eom, U. Bernhardt, K.R. Miller, S. Prokop, H. Kettenmann, and F.L. Heppner. 2013. Functional impairment of microglia coincides with beta-amyloid deposition in mice with Alzheimer-like pathology. *PLoS ONE.* 8:e60921. http://dx.doi.org/10.1371/journal.pone.0060921

Levites, Y., P. Das, R.W. Price, M.J. Rochette, L.A. Kostura, E.M. McGowan, M.P. Murphy, and T.E. Golde. 2006. Anti-Aβ42– and anti-Aβ40–specific mAbs attenuate amyloid deposition in an Alzheimer disease mouse model. *J. Clin. Invest.* 116:193–201. http://dx.doi.org/10.1172/JCI25410

Liu, C., G. Cui, M. Zhu, X. Kang, and H. Guo. 2014. Neuroinflammation in Alzheimer's disease: chemokines produced by astrocytes and chemokine receptors. *Int. J. Clin. Exp. Pathol.* 7:8342–8355.

Mildner, A., B. Schlevogt, K. Kierdorf, C. Böttcher, D. Erny, M.P. Kummer, M. Quinn, W. Brück, I. Bechmann, M.T. Heneka, et al. 2011. Distinct and non-redundant roles of microglia and myeloid subsets in mouse

models of Alzheimer's disease. *J. Neurosci.* 31:11159–11171. http://dx.doi.org/10.1523/JNEUROSCI.6209-10.2011

Naert, G., and S. Rivest. 2011. CC chemokine receptor 2 deficiency aggravates cognitive impairments and amyloid pathology in a transgenic mouse model of Alzheimer's disease. *J. Neurosci.* 31:6208–6220. http://dx.doi.org/10.1523/JNEUROSCI.0299-11.2011

Prokop, S., K.R. Miller, and F.L. Heppner. 2013. Microglia actions in Alzheimer's disease. *Acta Neuropathol.* 126:461–477. http://dx.doi.org/10.1007/s00401-013-1182-x

Radde, R., T. Bolmont, S.A. Kaeser, J. Coomaraswamy, D. Lindau, L. Stoltze, M.E. Calhoun, F. Jäggi, H. Wolburg, S. Gengler, et al. 2006. Aβ42-driven cerebral amyloidosis in transgenic mice reveals early and robust pathology. *EMBO Rep.* 7:940–946. http://dx.doi.org/10.1038/sj.embor.7400784

Simard, A.R., D. Soulet, G. Gowing, J.P. Julien, and S. Rivest. 2006. Bone marrow-derived microglia play a critical role in restricting senile plaque formation in Alzheimer's disease. *Neuron.* 49:489–502. http://dx.doi.org/10.1016/j.neuron.2006.01.022

Stalder, A.K., F. Ermini, L. Bondolfi, W. Krenger, G.J. Burbach, T. Deller, J. Coomaraswamy, M. Staufenbiel, R. Landmann, and M. Jucker. 2005. Invasion of hematopoietic cells into the brain of amyloid precursor protein transgenic mice. *J. Neurosci.* 25:11125–11132. http://dx.doi.org/10.1523/JNEUROSCI.2545-05.2005

Town, T., Y. Laouar, C. Pittenger, T. Mori, C.A. Szekely, J. Tan, R.S. Duman, and R.A. Flavell. 2008. Blocking TGF-β–Smad2/3 innate immune signaling mitigates Alzheimer-like pathology. *Nat. Med.* 14:681–687. http://dx.doi.org/10.1038/nm1781

Ulrich, J.D., M.B. Finn, Y. Wang, A. Shen, T.E. Mahan, H. Jiang, F.R. Stewart, L. Piccio, M. Colonna, and D.M. Holtzman. 2014. Altered microglial response to Aβ plaques in APPPS1-21 mice heterozygous for TREM2. *Mol. Neurodegener.* 9:20. http://dx.doi.org/10.1186/1750-1326-9-20

Varvel, N.H., S.A. Grathwohl, F. Baumann, C. Liebig, A. Bosch, B. Brawek, D.R. Thal, I.F. Charo, F.L. Heppner, A. Aguzzi, et al. 2012. Microglial repopulation model reveals a robust homeostatic process for replacing CNS myeloid cells. *Proc. Natl. Acad. Sci. USA.* 109:18150–18155. http://dx.doi.org/10.1073/pnas.1210150109

Varvel, N.H., S.A. Grathwohl, K. Degenhardt, C. Resch, A. Bosch, M. Jucker, and J.J. Neher. 2015. Replacement of brain-resident myeloid cells does not alter cerebral amyloid-β deposition in mouse models of Alzheimer's disease. *J. Exp. Med.* 212. http://dx.doi.org/10.1084/jem.20150478

Villeda, S.A., J. Luo, K.I. Mosher, B. Zou, M. Britschgi, G. Bieri, T.M. Stan, N. Fainberg, Z. Ding, A. Eggel, et al. 2011. The ageing systemic milieu negatively regulates neurogenesis and cognitive function. *Nature.* 477:90–94. http://dx.doi.org/10.1038/nature10357

vom Berg, J., S. Prokop, K.R. Miller, J. Obst, R.E. Kälin, I. Lopategui-Cabezas, A. Wegner, F. Mair, C.G. Schipke, O. Peters, et al. 2012. Inhibition of IL-12/IL-23 signaling reduces Alzheimer's disease-like pathology and cognitive decline. *Nat. Med.* 18:1812–1819. http://dx.doi.org/10.1038/nm.2965

Wang, A., P. Das, R.C. Switzer III, T.E. Golde, and J.L. Jankowsky. 2011. Robust amyloid clearance in a mouse model of Alzheimer's disease provides novel insights into the mechanism of amyloid-β immunotherapy. *J. Neurosci.* 31:4124–4136. http://dx.doi.org/10.1523/JNEUROSCI.5077-10.2011